$Na_V1.6a$ Is Required for Normal Activation of Motor Circuits Normally Excited by Tactile Stimulation

Sean E. Low,[1*] Weibin Zhou,[2†] Ingxin Choong,[2] Louis Saint-Amant,[2*] Shawn M. Sprague,[2] Hiromi Hirata,[2‡] Wilson W. Cui,[3§] Richard I. Hume,[1,2] John Y. Kuwada[1,2,3]

[1] Neuroscience Program, University of Michigan, Ann Arbor, Michigan 48109-1048

[2] Department of Molecular, Cellular and Developmental Biology, University of Michigan, Ann Arbor, Michigan 48109-1048

[3] Cell and Molecular Biology Program, University of Michigan, Ann Arbor, Michigan 48109-1048

Received 18 December 2009; revised 19 February 2010; accepted 4 March 2010

ABSTRACT: **A screen for zebrafish motor mutants identified two noncomplementing alleles of a recessive mutation that were named *non-active* (*nav^{mi89}* and *nav^{mi130}*). *nav* embryos displayed diminished spontaneous and touch-evoked escape behaviors during the first 3 days of development. Genetic mapping identified the gene encoding $Na_V1.6a$ (*scn8aa*) as a potential candidate for *nav*. Subsequent cloning of *scn8aa* from the two alleles of *nav* uncovered two missense mutations in $Na_V1.6a$ that eliminated channel activity when assayed heterologously. Furthermore, the injection of RNA encoding wild-type *scn8aa* rescued the *nav* mutant phenotype indicating that *scn8aa* was the causative gene of *nav*. *In-vivo* electrophysiological analysis of the touch-evoked escape circuit indicated that voltage-dependent inward current was decreased in mechanosensory neurons in mutants, but they were able to fire action potentials. Furthermore, tactile stimulation of mutants activated some neurons downstream of mechanosensory neurons but failed to activate the swim locomotor circuit in accord with the behavioral response of initial escape contractions but no swimming. Thus, mutant mechanosensory neurons appeared to respond to tactile stimulation but failed to initiate swimming. Interestingly fictive swimming could be initiated pharmacologically suggesting that a swim circuit was present in mutants. These results suggested that $Na_V1.6a$ was required for touch-induced activation of the swim locomotor network.** © 2010 Wiley Periodicals, Inc. Develop Neurobiol 70: 508–522, 2010

Keywords: **zebrafish; $Na_V1.6$; *scn8a*; motor behaviors**

INTRODUCTION

How the activity of genes, and the proteins they encode, contribute to behavior is a central question in neurobiology. To address this question forward genetic screens (Granato et al., 1996; Baier, 2000) have recently been coupled with *in-vivo* electrophysiological recordings in zebrafish (Drapeau et al., 1999; Buss and

Sean E. Low and Weibin Zhou contributed equally to this study.

**Present address:* Departement de Pathologie et Biologie Cellulaire, Universite de Montreal, Montreal, Quebec H3T IJ4.

†*Present address:* Life Science Institute, University of Michigan, Ann Arbor, Michigan 48109.

‡*Present address:* Graduate School of Science, Nagoya University, Nagoya 464-8602, Japan.

§*Present address:* Department of Anesthesia and Perioperative Care, University of California, San Francisco, California 94143.

Correspondence to: J.Y. Kuwada (kuwada@umich.edu).

Contract grant sponsor: National Institute of Neurological Disorders and Stroke; contract grant number: NS054731.

Contract grant sponsor: National Science Foundation; contract grant number: 0725976.

Contract grant sponsor: Center for Organogenesis Training Grant; contract grant number: 5-T32-HD007505.

Contract grant sponsors: National Institute of Neurological Disorders and Strokes, Fond de Recherche en Santé du Québec, International Human Frontier Science Program.

© 2010 Wiley Periodicals, Inc.

Published online 11 March 2010 in Wiley InterScience (www.interscience.wiley.com).
DOI 10.1002/dneu.20791

Drapeau, 2000). This combined approach has aided in the identification of several genes important for the formation and function of the networks that underlie zebrafish behaviors, in particular motor behaviors (Ono et al., 2002, 2004; Cui et al., 2004, 2005; Zhou et al., 2006; Hirata et al., 2004, 2005, 2007).

Within the first 2 days of development zebrafish embryos perform three highly stereotyped motor behaviors (Saint-Amant and Drapeau, 1998). Beginning at ~17 hours postfertilization (hpf) embryos exhibit spontaneous slow coiling of the trunk and tail. Spontaneous coiling is intrinsic to the spinal cord as it persists following spinalization. Later at ~21 hpf, embryos begin to respond to touch with fast and vigorous escape contractions. Lastly at ~28 hpf tactile stimulation evokes escape contractions followed by swimming. Spinalized embryos respond to tactile stimuli with an initial contraction, but subsequent contractions were dramatically reduced and no swimming occurred (Downes and Granato, 2006). By contrast, when embryos were transected between the midbrain and hindbrain, the trunk and tail displayed normal, alternating contractions indistinguishable from those of intact embryos and normal swimming (Saint-Amant and Drapeau, 1998). Thus, the intact hindbrain and spinal cord appear to be necessary and sufficient for the complete touch-evoked escape response and swimming, but the spinal cord may be sufficient for the initial contraction.

As previous mutagenesis screens failed to reach saturation, we undertook a forward genetic screen to identify additional behavioral mutants. From this screen two alleles of a mutation named *non-active* (*nav*) were identified. *nav* mutants displayed deficient spontaneous coiling and diminished touch-evoked behaviors. Subsequent cloning and rescue experiments demonstrated that the gene encoding $Na_V1.6a$ on chromosome 23 was the causative gene in *nav*. *In-vivo* electrophysiological analysis of the escape circuit in *nav* mutants revealed that tactile stimuli activated neurons downstream of mechanosensitive neurons suggesting that mechanosensory neurons were activated but failed to activate the locomotor network capable of generating swimming. However, swimming could be initiated pharmacologically suggesting that a swimming locomotor network was present in mutants. Thus, $Na_V1.6a$ was required for touch-induced activation of the swim locomotor network.

METHODS

Materials

Unless otherwise noted, reagents were obtained from Sigma Chemical (St. Louis, MO). Tetrodotoxin (TTX) and Riluzole were diluted to the indicated concentrations from stock solutions of 1 and 100 m*M*, respectively.

Animals

Zebrafish were bred and maintained according to approved guidelines set forth by the University Committee on Use and Care of Animals, University of Michigan. The two alleles of *non-active* (*nav*) nav^{mi89} and nav^{mi130} were isolated in a mutagenesis screen conducted at the University of Michigan using procedures previously reported (Haffter and Nusslein-Volhard, 1996). Prior to an experiment, zebrafish were dechorionated with pronase and developmentally staged as described previously (Kimmel et al., 1995).

Behavioral Analysis

Embryos obtained from crosses of *nav* heterozygous carriers were raised at 28.5°C. Spontaneous coiling was examined in dechorionated embryos at 21–22 hpf for 90 s each. The amplitude of a coil was measured as the angle that the caudal tip of the tail rotated starting from the longitudinal axis of the embryo. For example, when the tip of the tail touched the head the angle of rotation was 180°. The genotype of the embryos was subsequently determined by their response to touch. Touch-evoked behaviors were elicited by touching the tail with a fine tungsten wire (125 μm), or with the tips of a pair of No. 5 forceps. Motor behaviors were recorded by video microscopy using a Panasonic CCD camera (wv-BP330) attached to a Leica dissection microscope at 16–32× magnification. Images were captured (30 Hz) with a Scion LG-3 video card on a Macintosh G4 computer. The images and videos were analyzed offline with the Scion Image software and processed with ImageJ.

Mapping and Cloning of scn8aa

A mapping family for each allele was established by crossing a nav^{mi89} or nav^{mi130} female carrier (Michigan local strain) with a wild-type WIK male (Zebrafish Resource Center, Eugene, Oregon). One female and one male *nav* carrier were identified for each mapping family and used throughout the mapping process. Bulk segregate analysis (Postlethwait et al., 1994) was conducted according to the Zon lab protocol (http://zfrhmaps.tch.harvard.edu) using 20 wild-type sibling and 20 mutant embryos. Thereafter, eight wild-type siblings and 88 mutant embryos were subjected to intermediate resolution mapping using linked microsatellite (SSLP) markers identified from the bulk segregate analysis. For higher resolution mapping, 900 mutants were tested for the linked microsatellite marker Z4421 (http://zfin.org).

The *scn8aa* gene was physically mapped to the LN54 radiation hybrid panel by PCR (Hukriede et al., 1999). Primers were designed against the genomic contig Zv4_scaffold 1916 (http://www.ensembl.org/Danio_rerio/):

forward primer 5′-AAGCCGCCACCTAAGCCAGAC-3′;
reverse primer 5′-TGTTGCCACCATGCCAGGAG-3′.

To clone *scn8aa* total RNA was isolated from 27–30 hpf Michigan wild types or homozygous *nav* mutants using Trizol® reagent (Invitrogen, Carlsbad, CA). Total cDNA was synthesized using oligo-dT primers and Superscript II reverse transcriptase (Invitrogen, Carlsbad, CA) following the manufacturer's protocol (Superscript II manual, version 11-11-203). The coding sequence of *scn8aa* was cloned by PCR from wild-type and *nav* mutant cDNA using six pairs of PCR primers designed against the published zebrafish *scn8aa* sequence (NM_131628). PCR products were gel-purified and sequenced, or cloned into the pGEM®-T easy vector (Promega Madison, WI) prior to sequencing. Sequence analysis was performed using Lasergene software (DNAStar, Madison, WI).

Expression of scn8aa by *Xenopus oocytes*

Wild-type *scn8aa* template in pBluescript SK+ was provided by Dr. L.L. Isom (University of Michigan, Ann Arbor). Mutant *scn8aa* templates were obtained by subcloning a fragment encoding the *nav* mutations in place of wild-type sequence in the above construct. All mutations were confirmed by DNA sequencing (University of Michigan DNA Sequencing Core) and are referred to using the one letter code such as M1461K, which represents the substitution of methionine 1461 with a lysine.

Capped RNA encoding wild-type or mutant *scn8aa* was synthesized using the mMESSAGE mMACHINE® T3 kit (Ambion, Austin, TX). Defolliculated Stage V-VI *Xenopus* oocytes were injected with 12.5 ng of wild-type or mutant RNA diluted in 50 nL of DEPC-ddH_20 using a Nanoinject II system (Drummond Scientific Company, Broomall, PA). In some experiments oocytes were co-injected with 12.5 ng of RNA encoding the zebrafish β1 subunit. Following injection oocytes were maintained in Barth's solution at 17°C for 48–72 h before electrophysiological recordings. Two-electrode voltage clamp recordings were made with an NPI Electronics (Tamm, Germany) TurboTec 3 amplifier. The recording pipette solution contained 3 *M* KCl, and the oocyte external recording solution was as follows (in m*M*): 90 NaCl, 1 KCl, 1.7 MgCl2, and 10 HEPES, pH 7.6 (with NaOH). The oocyte external solution was controlled using a BPS-8 solution switcher (ALA Scientific Instruments, Westbury, NY). Experiments were performed at 22°C by holding oocytes at −100 mV, followed voltage steps to the indicated membrane potentials. Data acquisition and the switching of solutions were controlled by Clampex8.2 (Molecular Devices, Sunnyvale, CA) software using a Digidata 1322A interface (Axon Instruments, Union City, CA). Data analysis was performed using Clampfit 9 (Molecular Devices, Sunnyvale, CA), and figures were prepared using Sigma Plot 9.0 (SYSTAT Software, Chicago, IL).

To quantify the amplitude of the persistent current, an exponential function was first fit to the decay of the inward currents in response to a membrane depolarization from −100 to −30 mV. The percent persistent current was defined as the amplitude of current remaining five time constants after the peak current, divided by the amplitude of the peak current.

Mutant Rescue

For mutant rescue RNA encoding wild-type *scn8aa* was diluted to a concentration of 100 ng/μL in DEPC-ddH_20 containing 0.1% phenol red. Approximately 1.5 ng of RNA (visual assessment) was injected into each embryo at the 1–4 cell stage using a Picospritzer II (Parker Hannifin, Fairfield, NJ).

Whole-Mount *In-Situ* Hybridization and Immunolabeling

In-situ hybridization was carried out following standard lab protocols (Li et al., 2004). The antisense DIG-labeled probe for zebrafish *scn8aa* was made from the last 1.3 kb of coding sequence hydrolyzed to approximately <500 base pairs for application to embryos. After quenching the color reaction embryos were mounted in 70% glycerol/PBS and imaged with DIC microscopy.

The zn5 antibody (Trevarrow et al., 1990) recognizes the DM-GRASP Ig superfamily protein (Kanki et al., 1994; Fashena and Westerfield, 1999) and labels secondary spinal motor neurons in zebrafish (Beattie et al., 1997; Chandrasekhar et al., 1999). Zn5 (1:10 dilution) followed by Alexa488 tagged secondary antibody was applied to whole-mounted larvae at 66 hpf following previously published protocols (see references above). Larvae were mounted in 75% glycerol and imaged with epifluorescence on a upright compound microscope.

In Vivo Electrophysiology

Embryos (48–52 hpf) were prepared for *in vivo* recordings from axial skeletal muscle and motor neurons as previously described (Ribera and Nusslein-Volhard, 1998; Drapeau et al., 1999; Buss and Drapeau 2000). In brief embryos were anesthetized in 1× Evans recording solution (in m*M*): 134 NaCl, 2.9 KCl, 2.1 $CaCl_2$, 1.2 $MgCl_2$, 10 glucose, 10 HEPES, pH 7.8, containing 0.02% tricaine. Embryos were then pinned to a 35-mm dish coated with Sylgard® through the notochord using 25 μm tungsten wires. The skin overlying the trunk and tail was first scored with a broken pipette, and then removed with a pair of fine No.5 forceps. The bath solution was continuously exchanged at ~1 mL/min throughout the recording session with 1× Evans for Mauthner cell recordings, 1× Evans containing 2–3 μM D-tubocurarine for muscle recordings, or 15 μM for Rohon-Beard (RB) and motor neuron recordings. The internal recording solution contained (in m*M*): 116 K-gluconate, 16 KCl, 2 $MgCl_2$, 10 HEPES, 10 EGTA, at pH 7.2 with 0.1% sulforhodamine B for cell type identification. Electrodes pulled from Borosilicate glass had resistances of 6–10 MΩ for muscle, 10–14 MΩ for RB and motor neurons when filled with internal recording solution, and ~1 MΩ when filled with external recording solution for Mauthner cell record-

ings. To expose the spinal cord for motor neuron and Rohon-Beard recordings, the bath solution was replaced with recording solution containing 2 mg/mL collagenase Type XI and incubated at room temperature (22°C) until the axial skeletal muscle started to separate at the somitic boundaries. Thereafter, the muscle was peeled away using suction applied to a broken pipette (~50 μm). Recordings were made with an Axopatch 200B amplifier (Axon Instruments, Union City, CA) low-passed filtered at 5 kHz and sampled at 1–10 kHz. Data acquisition using a Digidata 1322A interface was controlled by pClamp 8.2 software. The initial data analysis was done with Clampfit 9.2, and figures were prepared using Sigma Plot 9.0.

Touch-evoked responses were evoked by pressure application of bath solution via a broken pipette (~20 μm) to the tail region. The pressure and duration of a stimulus was controlled by a Picospritzer II. NMDA-evoked fictive swimming was achieved by perfusing the bath with recording solution containing 100 μM NMDA.

RESULTS

nav Mutants Exhibit Abnormal Touch-Evoked Behaviors

Two recessive motor mutants were identified from an ENU-induced mutagenesis screen for behavioral mutations. The behavioral phenotype of the two mutants was similar and complementation analysis revealed that the two mutants were allelic and were collectively named *non-active* (nav^{mi89} and nav^{mi130}). At 21 hpf spontaneous coiling was both lower in frequency and amplitude in *nav* mutants compared with wild-type siblings [Fig. 1(A,B)]. During the second and third day of development, mutants displayed diminished touch-evoked behaviors. By ~24 hpf when wild-type siblings typically responded to tactile stimuli with two or more fast, escape contractions, *nav* mutants most frequently responded with fewer escape contractions that were less vigorous [Fig. 1(C,D)]. Later at ~48 hpf when wild-type siblings normally responded to touch with escape contractions followed by swimming, *nav* mutants performed only escape contractions with no swimming [Fig. 1(E)]. Thus, *nav* mutants were able to detect tactile stimuli, but responded with diminished escape behaviors. Interestingly *nav* mutants eventually gained the ability to swim in response to touch by ~60 hpf [Fig. 1(F)], but they did not survive beyond 2 weeks.

There Is a Defect in the Nervous System of *nav Mutants*

To better understand the genesis of the *nav* phenotype, touch-evoked activity within the zebrafish escape circuit was examined [Fig. 2(A)]. Sensitivity to touch in zebrafish was conferred by two groups of mechanosensitive neurons: those within the trigeminal ganglia relayed tactile stimuli to the head, whereas Rohon-Beard neurons (RBs) located within the dorsal spinal cord relayed tactile stimuli to the trunk and tail. Both groups of mechanosensitive neurons projected axons into the hindbrain (Metcalfe et al., 1990) to activate ~90 pairs of reticulospinal neurons including the Mauthner (M) cell during escape behaviors (Gahtan et al., 2002). The M cell in turn made monosynaptic contacts with several spinal cord neurons including motor neurons (Jontes et al., 2000) to activate skeletal muscles resulting in locomotion.

As a first level of characterization touch-evoked activity was examined in axial skeletal muscles of the trunk. Axial skeletal muscle in zebrafish was comprised of slow and fast twitch fibers, both of which were active during swimming (Buss and Drapeau, 2002). Touch resulted in episodes of rhythmic membrane depolarizations that underlie swimming in slow twitch fibers of wild-type siblings [$n = 5$; Fig. 2(B)] similar to previous reports (Buss and Drapeau, 2002). In contrast short, arhythmic depolarizations were observed in *nav* slow twitch fibers in response to touch ($n = 5$). The aberrant responses of muscles in *nav* mutants were consistent with touch-evoked escape contractions, but no swimming in *nav* mutants.

The abnormal touch-evoked response of *nav* muscles could be a result of a defect within the nervous system, or a defect in skeletal muscle that disrupts muscle's ability to respond to sustained input from motor neurons. To determine whether the output of the CNS was defective in *nav* mutants, touch-evoked activity in motor neurons was examined. Recordings made from all three primary motor neurons (CaP, MiP, and RoP) revealed that touch evoked a prolonged burst of action potentials in wild-type embryos [$n = 5$; Fig. 2(C)] similar to previous reports (Buss and Drapeau, 2001). In contrast, touch evoked only a short burst of action potentials in primary motor neurons of *nav* mutants ($n = 5$), consistent with the abbreviated response of skeletal muscles. Thus, tactile stimuli were not properly converted into a normal motor output by the nervous system of *nav* mutants.

Touch Triggers Activity by the Mauthner Cell Within the Escape Circuit of *nav* Mutants

In fish the M cells are reticulospinal interneurons that receive input from mechanosensitive neurons (Zottoli and Faber, 1979), and in turn make monosynaptic

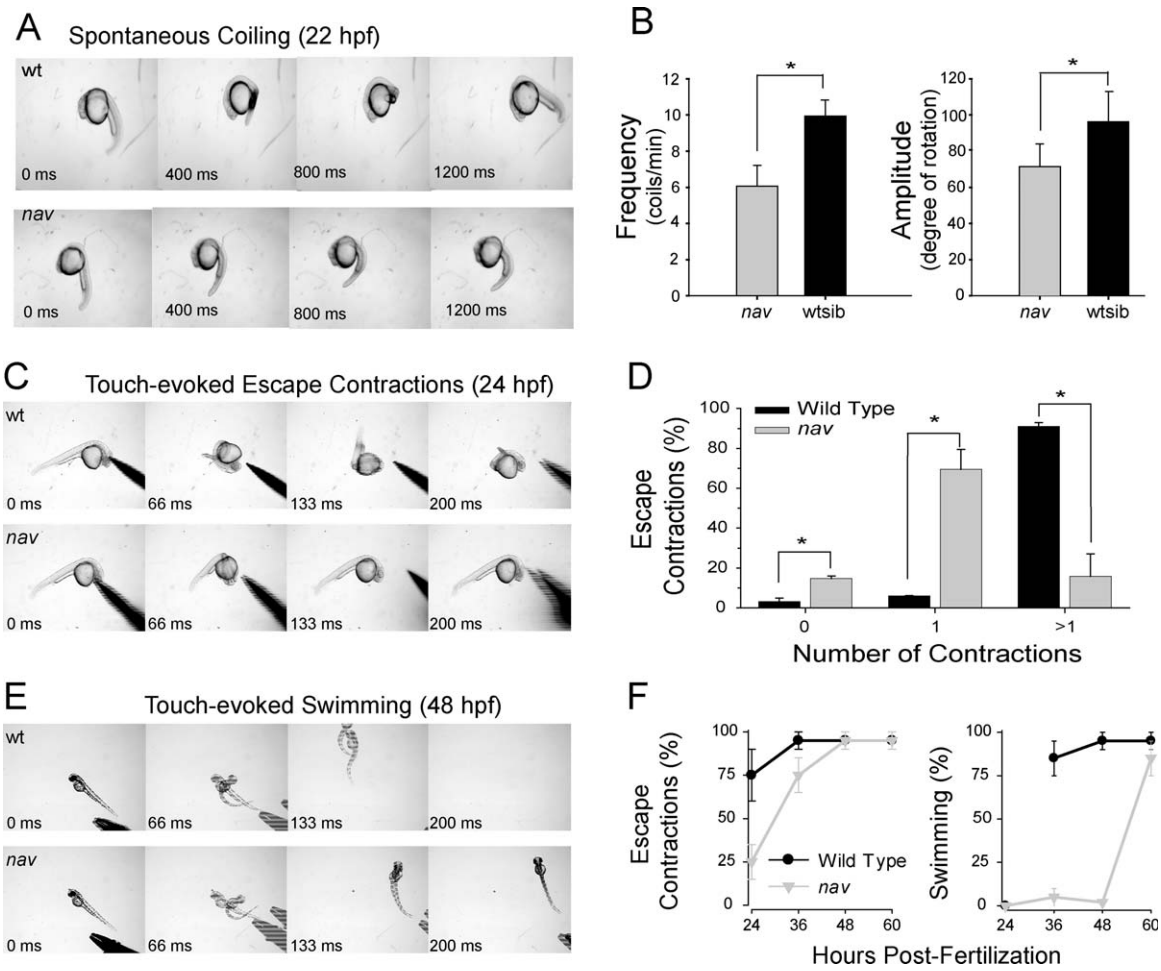

Figure 1 *nav* mutants exhibit abnormal spontaneous coiling amplitude, and diminished touch-evoked behaviors. (A) Top: a 22-hpf wild-type sibling exhibiting a single spontaneous coil. Bottom: an aged-matched *nav* mutant embryo exhibiting a weaker spontaneous coil when compared to wild-type sibs. (B) Frequency (left) and amplitude (right) of the spontaneous coils (angle of rotation of the tail) of wild-type sib ($n = 33$) were greater than that of *nav* mutant ($n = 12$) embryos at 21 hpf (*t* test: $p < 0.01$ for frequency; $p < 0.05$ for amplitude). (C) Top: a 24-hpf wild-type sibling touched on the head responds with multiple escape contractions. Bottom: an aged-matched *nav* mutant embryo responds with a single contraction. (D) Percent of touch-evoked escape contractions consisting of no contractions, one contraction and greater than one contraction in wild-type ($n = 30$) and *nav* mutant ($n = 30$) embryos at 24 hpf. All differences (asterisks) were significantly different (*t*-test: $p < 0.05$). (E) Top: a 48-hpf wild-type sibling touched on the tail responds with an escape contraction followed by swimming. The embryo appears twice in some frames as the behavior was faster than the video capture rate. Bottom: an aged-matched *nav* mutant responds with an escape contraction but no swimming. (F) Progression of the *nav* phenotype over the first few days of development compared to wild type. Values represent the average ± SEM escape response displayed by either wild-type or mutant embryo groups ($n = 3$ groups each, 25 embryos each group).

contacts with motor neurons (Jontes et al., 2000) [Fig. 2(A)]. Activity in M cells follows sensory stimulation (Zottoli, 1977), precedes the onset of escape contractions (Eaton et al., 1988), and is sufficient to trigger a weaker and less variable escape contraction compared with that initiated by tactile stimulation (Nissanov et al., 1990). Furthermore, ~90 reticulospinal neurons are known to be activated during escape behaviors suggesting that a full-fledge escape response is mediated by the M cell and numerous other reticulospinal interneurons (Gahtan et al., 2002). To examine whether the M cell is activated by tactile stimulation focal, extracellular recordings were used to monitor their spiking activity (Eaton

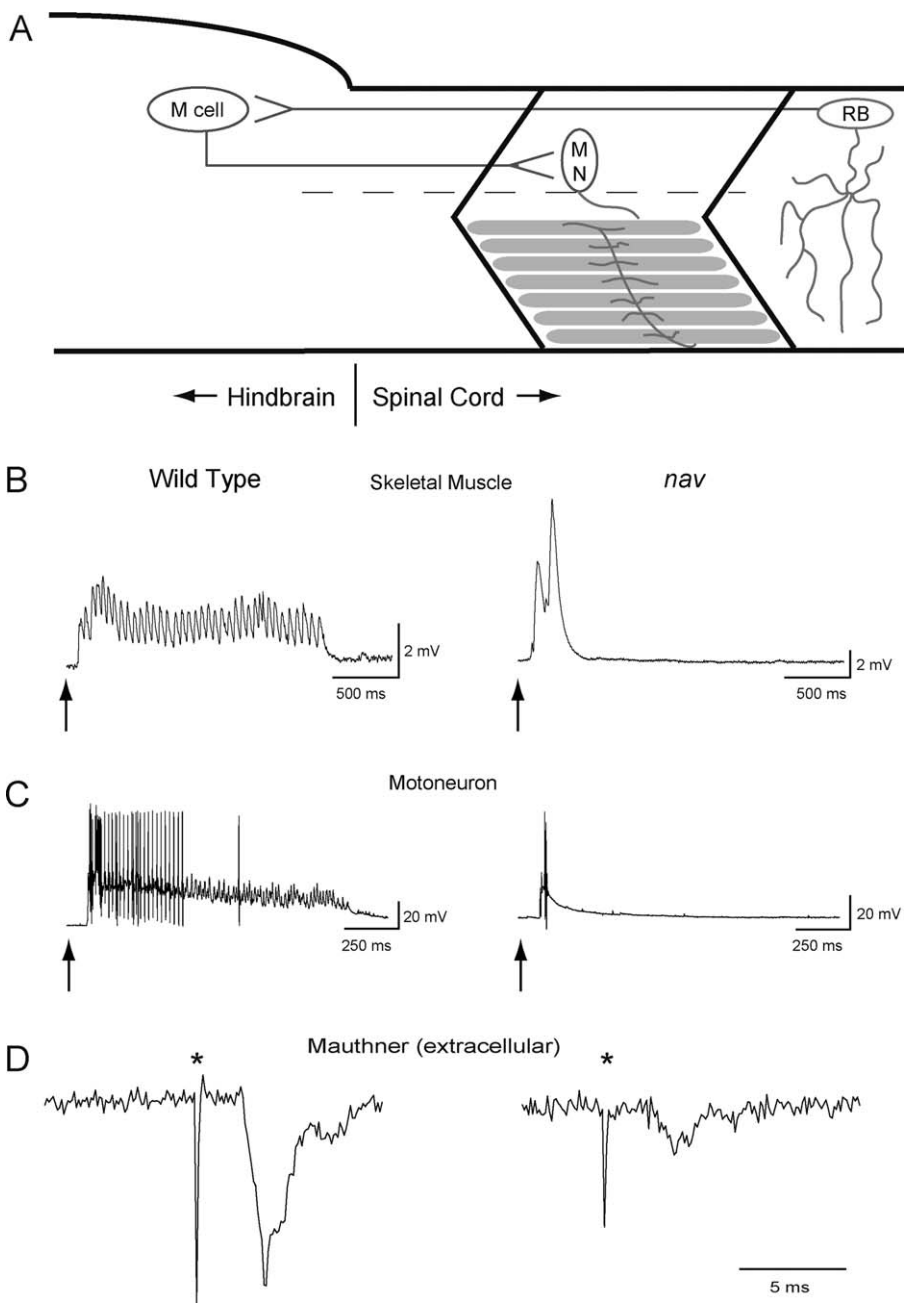

Figure 2 Tactile stimulation induces abbreviated bouts of touch-evoked activity in muscle and motor neurons but normal activation of M cells in *nav* mutants. (A) A schematic depicting the simplest neural circuit mediating escape contractions. Sensory input from the mechanosensitive RB neurons activate M cells, which make monosynaptic contacts with motor neurons (MN) that innervate axial skeletal muscle. (B) A prolonged bout of touch-evoked fictive swimming is observed in skeletal muscle of wild-type siblings ($n = 5$), while an arrhythmic abbreviated response is recorded in *nav* mutants ($n = 5$). Arrows here and in panel (C) indicate the approximate time of stimulus. (C) Prolonged bouts of touch-evoked bursting in primary motor neurons are observed in wild-type sibling ($n = 5$), but not in *nav* mutant ($n = 5$) embryos. (D) Touch-evoked M cell spiking recorded extracellularly from wild-type sibling (left, $n = 5$) and *nav* mutant (right, $n = 5$) embryos. (*) denotes M cell spiking followed by an electromyogram (EMG). Of note, the amplitude of extracellular activity varies with respect to the location of the recording electrode.

and Farley, 1975). Such records reveal that touch evokes spiking by M cells of both wild-type siblings ($n = 5$) and *nav* mutants ($n = 5$) at 48–52 hpf [Fig. 2(D)]. Thus, sensory information is capable of activating the M cell in mutant embryos to initiate escape responses albeit diminished ones. Since the weaker escape response of *nav* mutants is reminiscent of escape responses induced by direct stimulation of the M cells, it may be possible that many of the other reticulospinal interneurons normally activated by tactile stimulation may fail to do so in *nav* mutants.

RBs *in nav* Mutants Exhibit Reduced Sodium Currents

Tactile stimuli likely activated mechanosensory neurons in *nav* mutants since the M cell is activated and mutants respond to touch albeit with a diminished response. However, it is still possible that the response of mechanosensory neurons although sufficient to activate the M cell in mutants may not be able to activate other reticulospinal interneurons that may normally be activated in a full-fledge escape response. To see if diminished touch-evoked behaviors might be explained by reduced excitability of mechanosensory neurons, RBs were examined by whole-cell voltage and current clamp recordings between 48 and 52 hpf. In wild-type RBs, membrane depolarization evoked a rapidly activating-inactivating inward current (3.04 ± 0.16 nA, $n = 12$), followed by a prolonged outward current [Fig. 3(A,B)]. The application of TTX to the bath blocked all the inward current ($n = 3$, not shown) consistent with the reported TTX sensitivity of voltage-gated sodium channels expressed by RBs (Pineda et al., 2005). In RBs of *nav* mutants membrane depolarizations also evoked inward currents in all RBs examined. However, the average peak inward current in mutant RBs was reduced to approximately 70% of wild type (2.12 ± 0.35 nA, $n = 12$; *t*-test, $p < 0.05$). The voltage-gated outward currents were comparable between wild type and mutants: the peak I_{out} at $V_{hold} = +80$ mV for wt was 3108 ± 256 pA and for *nav* was 2522 ± 382 pA (*t*-test, $p = 0.22$). When studied under current clamp conditions, short depolarizing current injections resulted in a single overshooting action potential in wild-type ($n = 10$) RBs [Fig. 3(C)], and prolonged (100 ms) supratheshold current pulses elicited a single action potential but failed to generate trains of action potentials (not shown). This suggested that RBs are unlikely to respond to tactile stimulation with a train of spikes. Interestingly, current injections into RBs from *nav* mutants ($n = 8$) also elicited a sin-

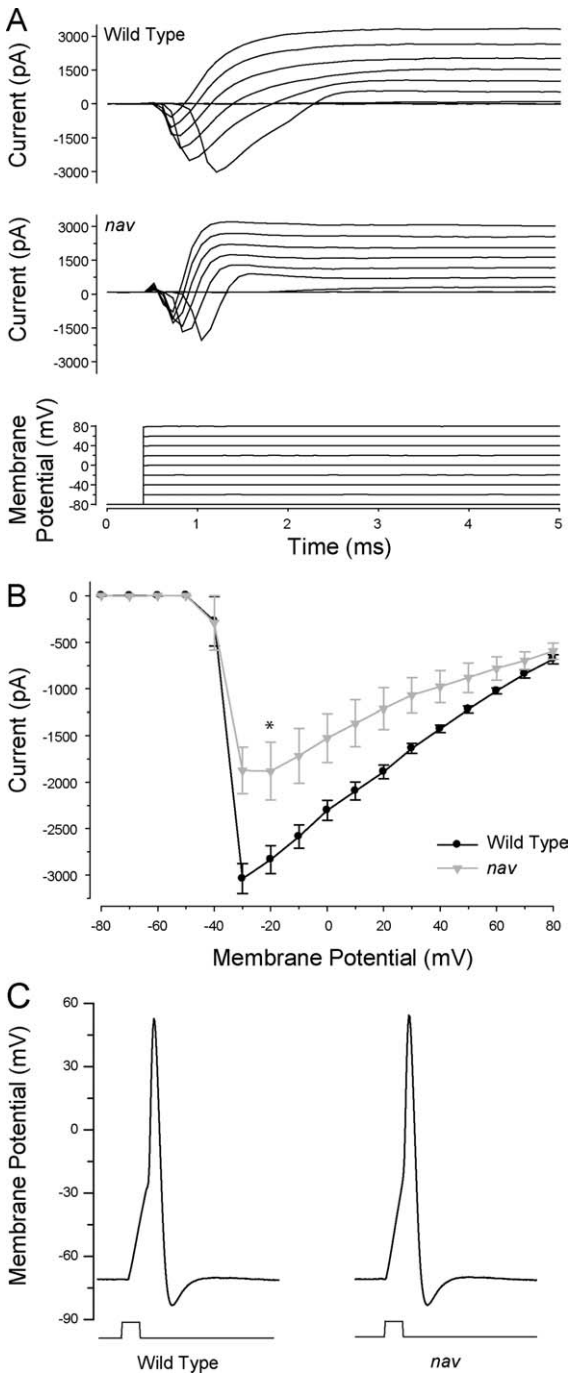

Figure 3 *nav* RBs exhibit decreased voltage-gated sodium currents, but retain the ability to generate overshooting action potentials. (A) Whole-cell current responses recorded in wild-type and *nav* mutant RBs (48–52 hpf) following membrane depolarizations. (B) Peak inward current plotted as a function of the membrane potential. Values represent the average ± SEM ($n = 12$ for wild type, and $n = 12$ for mutant). * denotes that difference between wild type and mutant was significant (*t*-test, $p < 0.05$). (C) Action potentials in wild-type and *nav* RBs evoked by depolarizing current injections (2 ms) shown below.

gle action potential. These findings demonstrated that although RBs in *nav* mutants exhibited diminished voltage-gated sodium currents, they retained the ability to fire action potentials, and suggested that the properties of neurons postsynaptic to sensory neurons may also be affected in mutants.

Fictive Swimming Can be Generated by *nav* Mutants

Analysis of the *nav* touch-evoked escape circuit revealed that mutants detected tactile stimuli, activated the M cell and initiated escape responses at 48 hpf. Yet tactile stimuli failed to initiate swimming in *nav* mutants. This could be due to a defective swimming circuit or a failure to activate the swim circuit. To discern between these two possibilities fictive swimming was driven within the locomotor network by the application of NMDA, which induced fictive swimming that was similar to tactile stimuli in zebrafish (Cui et al., 2004). NMDA (100 μM) evoked repetitive bouts of fictive swimming in both wild-type ($n = 5$) and mutant ($n = 5$) embryos [Fig. 4(A,B)]. Thus, an operational swimming circuit was present in mutants suggesting that the lack of touch-induced swimming in mutants may be due to deficient activation of the swim circuit in mutant embryos. However, the duration and intra-burst frequency but not the period of NMDA induced fictive swimming episodes in *nav* mutants were decreased compared to wild-type siblings [Fig. 4(C,D)]. Thus, the mutation also affected some parameters of the swim circuit, but the lack of any swimming response to mechanical stimulation in mutants suggested that the swim circuit was not properly activated.

nav Phenotype Arises from Missense Mutations in the Gene Encoding $Na_V1.6a$ (scn8aa) that Abolish Channel Activity

Meiotic mapping showed that microsatellite marker z4421 failed to recombine with either allele (0/1140 meioses). Microsatellite marker z4421 was located on chromosome 23 near the *scn8aa* gene that encoded for the voltage-gated sodium channel $Na_V1.6a$. Since mutations in mouse *scn8a* exhibited a range of movement defects (Meisler et al., 2002) reminiscent of the *nav* phenotype, zebrafish *scn8aa* cDNA was cloned and sequenced from nav^{mi89} and nav^{mi130} to see if they harbor mutations. Indeed the predicted amino acid sequences of $Na_v1.6a$ from nav^{mi89} and nav^{mi130} revealed M1461K and L277Q missense mutations, respectively [Fig. 5(A)]. These mutations occurred at highly conserved residues in $Na_V1.6$, and in the family of voltage-gated sodium channels as a whole.

To examine the functional consequences of these mutations, RNA from wild-type or mutant *scn8aa* were expressed in *Xenopus* oocytes and studied under two-electrode voltage-clamp. Although wild type *scn8aa* produced voltage-gated sodium currents similar to previous reports for zebrafish $Na_V1.6a$ (Fein et al., 2007), nav^{mi89} mutant *scn8aa* RNAs failed to produce currents different from uninjected oocytes [Fig. 5(B)]. Similarly oocytes injected with nav^{mi130} RNA generated no currents beyond those found in uninjected oocytes (not shown). To more accurately recapitulate conditions *in vivo*, mutant *scn8aa* RNAs were also co-injected with RNA encoding the zebrafish $\beta 1$ subunit, which promotes membrane insertion of voltage-gated sodium channels (Isom et al., 1995). Again no voltage-dependent currents different from uninjected oocytes were observed (not shown). Therefore, the two missense mutations in nav^{mi89} and nav^{mi130} both resulted in nonfunctional $Na_V1.6a$ channels.

To confirm that *scn8aa* was the causative gene in *nav* mutants, RNA encoding wild-type *scn8aa* was injected into recently fertilized embryos from a cross between two heterozygotes in an attempt to rescue the *nav* phenotype. Injection of wild-type RNA resulted in a reduction in the percent of embryos at 27 hpf that exhibited the mutant phenotype from the predicted Mendelian ratio of 25–15.6% (28/180). To see if mutants were indeed rescued, these injected embryos were assayed again at 48 hpf when the effect of the injected wild-type *scn8aa* RNA might have worn off. In fact at 48 hpf 26.7% (48/180) of the injected embryos displayed the *nav* phenotype. Therefore, 20 of the 180 embryos ($\chi^2 < 0.005$, $n = 180$) that exhibited normal touch-evoked escape behaviors at 27 hpf were *nav* mutants, but displayed a wild-type phenotype as a result of the injected wild-type *scn8aa* RNA. Thus, the *nav* phenotype was due to mutations in *scn8aa* that disrupted $Na_V1.6a$.

scn8aa Is Widely Expressed in the Zebrafish Nervous System

To better understand how the loss of $Na_V1.6a$ resulted in diminished touch-evoked responses in *nav* mutants, the expression pattern of *scn8aa* was examined at 24 and 48 hpf. Whole-mount *in situ* hybridization demonstrated that *scn8aa* was expressed in many early neurons in the spinal cord and brain at 24 hpf but not in muscles, consistent with previous reports (Pineda et al., 2005, 2006; Novak et al., 2006a; Chopra et al., 2007; Chen et al., 2008). The size and

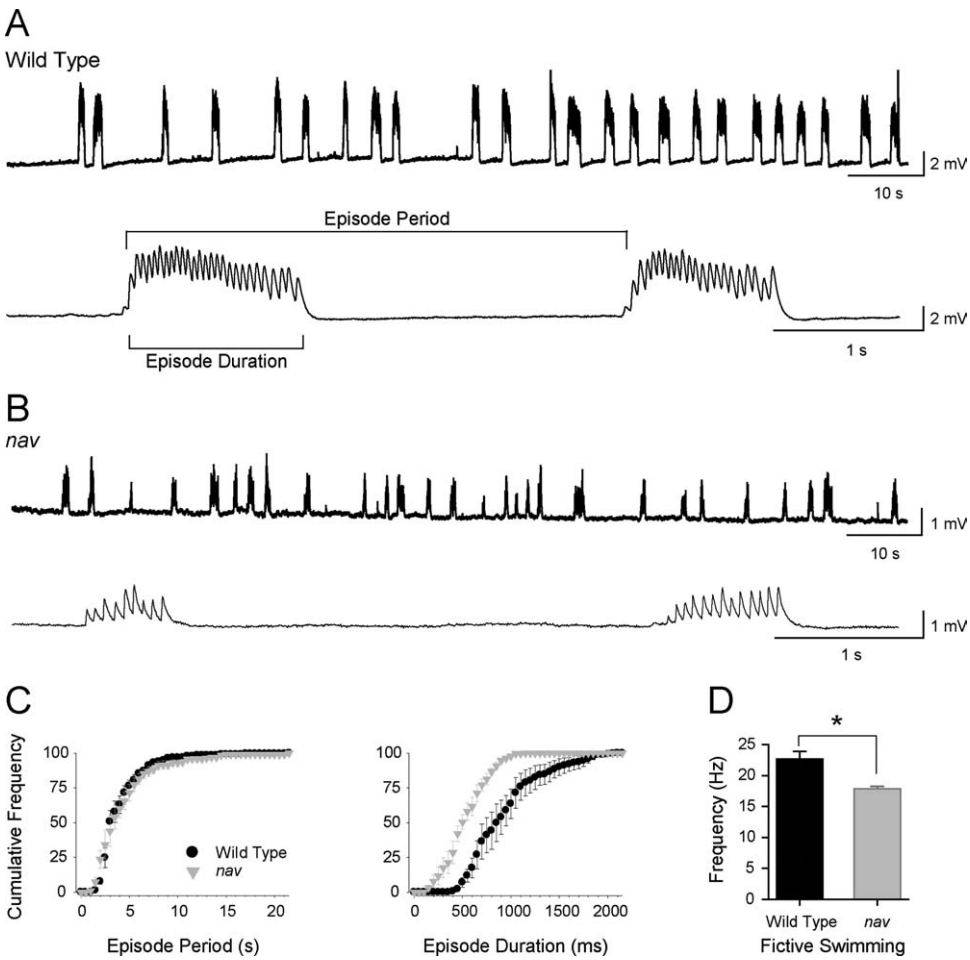

Figure 4 Abbreviated fictive swimming can be evoked by NMDA in *nav* mutants (48–52 hpf). (A) Top: intracellular voltage recordings showing several minutes of NMDA-evoked fictive swimming from a wild-type muscle fiber. Bottom: a faster sweep of two episodes of fictive swimming. (B) Top: intracellular voltage recordings showing several minutes of NMDA-evoked fictive swimming from a *nav* mutant fiber. Bottom: a faster sweep of two episodes of fictive swimming. (C) Cumulative frequency plots (left) of episode periods from wild-type siblings and *nav* mutant embryos ($n = 5$ for each) reveals no difference in how often episodes of fictive swimming are initiated. Cumulative frequency plots (right) of episode durations from wild-type siblings and *nav* mutant embryos ($n = 5$ for each) reveals that mutants typically swim for a shorter duration. (D) Fictive swimming frequency in *nav* mutants is slower when compared to wild-type sibling ($*p < 0.05$).

positions of some of the *scn8aa*-positive neurons suggested that they were likely posterior lateral line ganglion cells, trigeminal neurons and RB neurons [Fig. 6(A,B)]. At 48 hpf *scn8aa* was expressed widely within the CNS and PNS including sensory neurons [Fig. 6(C,E)]. Thus, expression of $Na_V1.6a$ by mechanosensory neurons and other neurons in the hindbrain and spinal cord was consistent with the observed physiological effects of the loss of $Na_V1.6a$ activity on touch-evoked responses.

Interestingly dorsally projecting motor neurons expressed *scn8aa* and development of these motor neurons was defective when $Na_V1.6a$ was knocked down (Pineda et al., 2006). By 66 hpf control larvae had developed the dorsal motor branch, but antisense Morpholino injected larvae had not. However, 66 hpf *nav* mutants exhibited dorsal motor branches comparable to that in wildtype sibs [Fig. 6(F,G)]. Dorsal branches labeled with zn5 antibody (see Methods) were examined in segments 5–15 in nine wild-type sibs and 10 *nav* mutants. Dorsal motor branches were found in 91% (181/198) of the hemisegments in wild-type sibs and 95% (209/220) of the hemisegments in *nav* mutants. Thus, the genetic loss of $Na_V1.6a$ activity appears not to be of consequence for the projection of the dorsal motor branch.

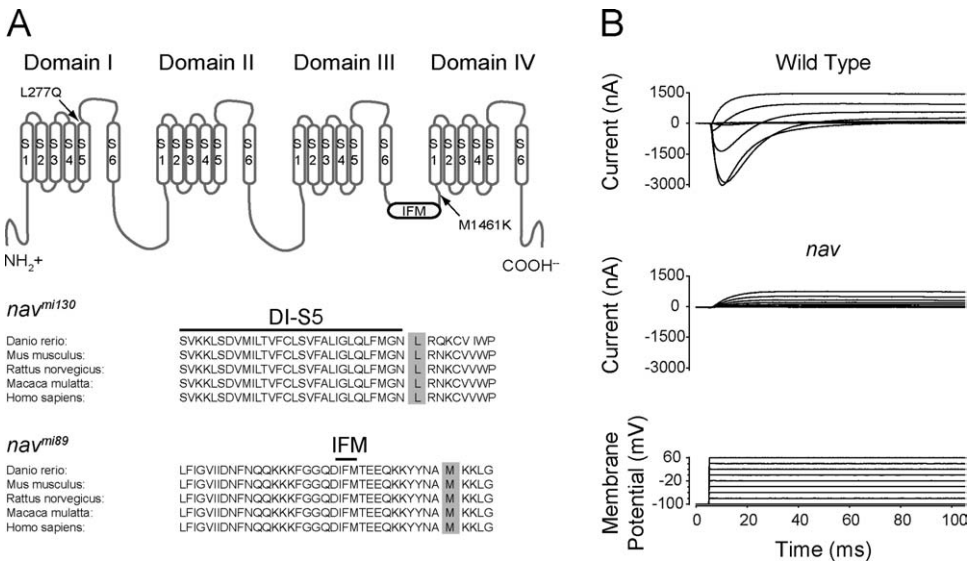

Figure 5 Missense mutations found in $Na_V1.6a$ from *nav*^{mi130} and *nav*^{mi89} abolish channel activity. (A) Top: $Na_V1.6a$ membrane topology and location of *nav* missense mutations. Bottom: sequence alignment of $Na_V1.6a$ from several different species with the conserved leucine 277 and methionine 1461 highlighted in gray. (B) Two electrode voltage-clamp recordings made from oocytes injected with either wild type or *nav*^{mi89} RNA. Of note oocytes exhibited variable endogenous outward currents.

nav Phenotype Correlates with a Loss of Persistent Sodium Current

Although voltage-gated sodium channels are best known for contributing to the rising phase of action potentials in muscle and neurons, a few members, including $Na_V1.6$, exhibit a non-inactivating persistent current ($I_{Na}p$) (Crill, 1996; Raman et al., 1997). Interestingly $I_{Na}p$ is essential for normal fictive locomotion in neonatal rodents (Tazerart et al., 2007; Zhong et al., 2007). Since *nav* mutants fail to initiate swimming following tactile stimulation, the role of $I_{Na}p$ for touch-induced swimming was examined. First, zebrafish $Na_V1.6a$ was examined to see if it exhibits $I_{Na}p$ by coexpressing RNA encoding $Na_V1.6a$ and the $\beta 1$ subunit in *Xenopus* oocytes and studying currents under two-electrode voltage clamp. In response to membrane depolarization a pronounced $I_{Na}p$ was observed [Fig. 7(A)].

Since $I_{Na}p$ in other organisms was sensitive to the drug Riluzole (Urbani and Belluzzi, 2000), the action of Riluzole was examined on $I_{Na}p$ exhibited by zebrafish $Na_V1.6a$. Riluzole preferentially blocked $I_{Na}p$ with minimal effects on transient peak current [Fig. 7(A,B)]. As a first step to determine whether a lack of $I_{Na}p$ might be involved in the *nav* phenotype, the behavior of embryos exposed to Riluzole was examined. Within several minutes of exposure to 10 μM Riluzole wild-type embryos (48 hpf) responded to touch with escape contractions but no swimming much like *nav* mutants [Fig. 7(C)]. The lack of swimming in 10 μM Riluzole treated wild-type embryos was due to a touch-induced abbreviated, arhythmic depolarization in muscles similar to that seen in *nav* mutants [Fig. 7(D)]. Further experiments are needed to clarify these initial findings, but the results raise the possibility that persistent sodium current is important for the transformation of transient tactile stimuli into prolonged motor behaviors in zebrafish.

DISCUSSION

A forward genetic screen in zebrafish uncovered two alleles of a behavioral mutation that was named *non-active* (*nav*). Both alleles of *nav* exhibited diminished spontaneous coiling similar to that described for $Na_V1.6a$ morphants (Tsai et al., 2001) and touch-evoked behaviors during the second and third days of development as a result of missense mutations in the gene encoding $Na_V1.6a$ (*scn8aa*) that abolished channel activity.

Skeletal muscles and motor neurons in *nav* mutants responded to tactile stimulation, but the response was of shorter duration compared to wild type siblings. This and the fact that *scn8aa* was not expressed by skeletal muscles (Tsai et al., 2001;

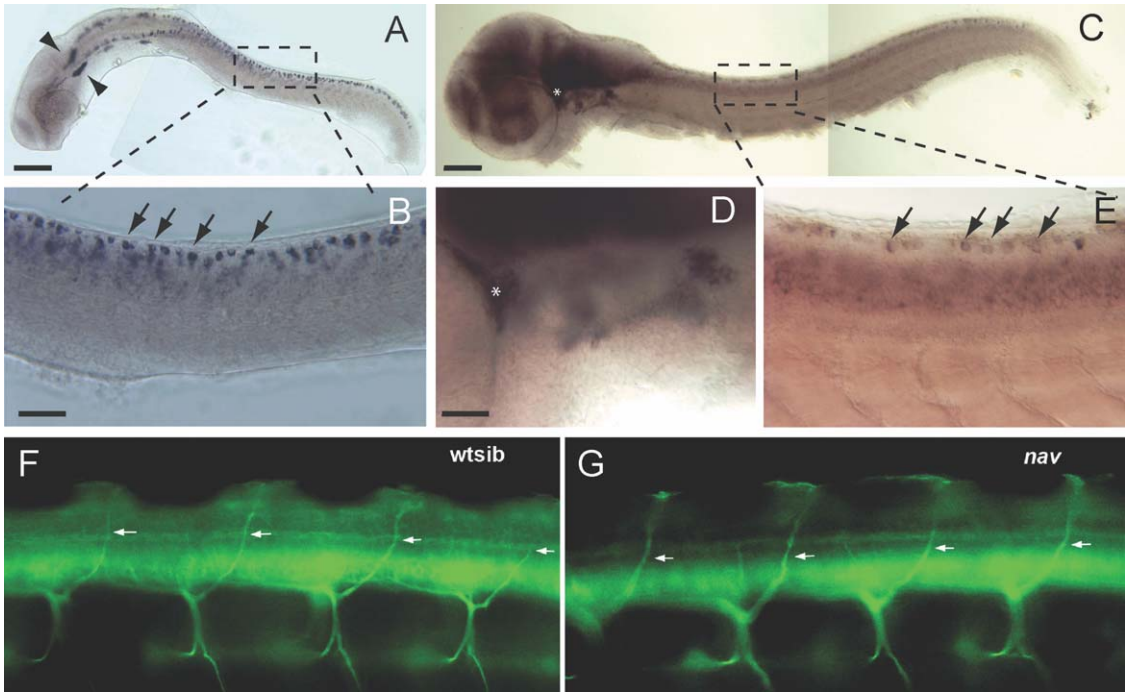

Figure 6 *scn8aa* is widely expressed within the CNS and PNS and motor nerves develop normally in *nav* mutants. (A) Expression of *scn8aa* in a 24-hpf embryo by the posterior lateral line ganglion (arrowheads) and RB neurons. Scale bar, 200 μm. (B) Enlarged image of region indicated in the top panel showing presumptive RB neurons (arrows highlight a few) expressing *scn8aa*. Scale bar, 50 μm. (C) Expression of *scn8aa* in a 48-hpf embryo is more widespread. Asterisk denotes the trigeminal ganglion that is shown at higher power in (D). Boxed area highlights RBs shown in (E). (D) Enlarged image of region containing the trigeminal ganglion that was denoted by an asterisk in (C). (E) Presumptive RBs (right, arrows highlight a few) expressing *scn8aa*. (F) Side view of the mid-trunk focused on the dorsal branches of the motor nerves (arrows) in a wild type sibling. Motor nerves were labeled with MAb Zn5 at 66 hpf. (G) Sideview of the mid-trunk showing normal dorsal branches of the motor nerves (arrows) in a *nav* mutant at 66 hpf. Anterior is to the left and dorsal up in both panels.

Novak et al., 2006b) demonstrated that the *nav* behavioral defect was a consequence of abnormal activity within the nervous system. Although zebrafish motor neurons do express *scn8aa* (Tsai et al., 2001; Novak et al., 2006b; Pineda et al., 2006), the expression of *scn8aa* has been detected only in a subset of motor neurons: the ventrally projecting CaP primary motor neuron, and the dorsally projecting secondary motor neurons. As our recordings were made from all three types of primary motor neurons (CaP, MiP, and RoP) and they all exhibited similar patterns of abbreviated bursting, a defect upstream of the motor neurons likely existed in *nav* mutants. In addition, the finding that NMDA evoked fictive swimming in *nav* mutants suggested that mutant motor neurons were capable of providing sustained drive to skeletal muscle when they received adequate synaptic stimulation. Thus, the lack of swimming in *nav* mutants involves a defect to neurons that were presynaptic to the motor neurons. Consistent with these findings, the development of motor nerves was unaffected by the loss of $Na_V1.6a$ activity in *nav* mutants. Previously $Na_V1.6a$ morphants were shown to exhibit defective development of the dorsal branch of the spinal motor nerve (Pineda et al., 2006). The reason for the difference between the *nav* and the morphant results is unclear, but one possibility is that genetic compensation such as by other Na_Vs may occur in *nav* mutants.

The finding that RB neurons can generate action potentials in *nav* mutants despite a decrease in voltage-dependent inward current, and that tactile stimulation activated M cells in mutants suggested that RB neurons do respond to tactile stimulation. One possible explanation for the *nav* phenotype might be that RBs may normally respond to tactle stimuli with a train of action potentials, and that the loss of $Na_V1.6a$ might lead to reduce the response to a single spike or shorter burst of spikes. The shortened response of

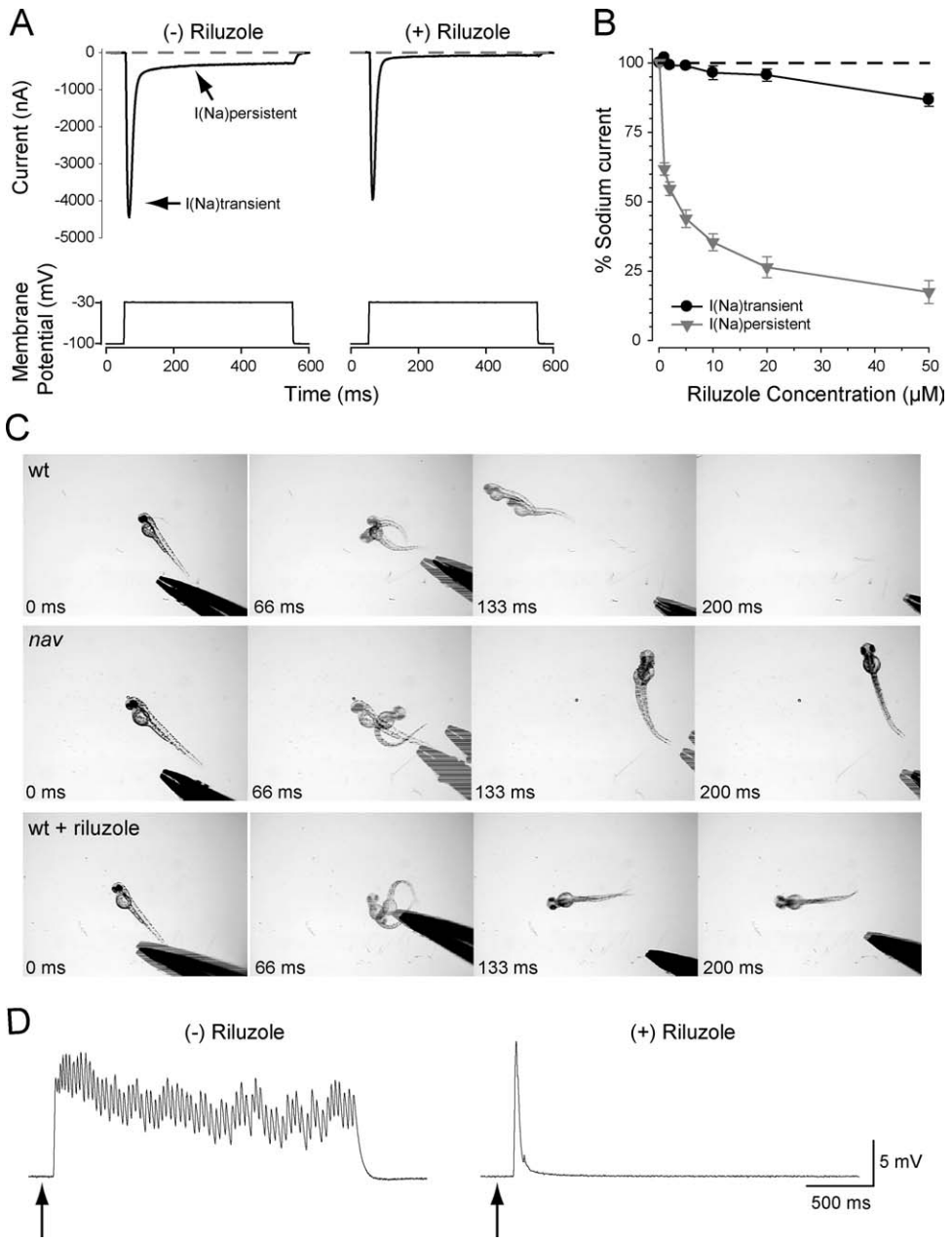

Figure 7 Riluzole preferentially blocks $Na_V1.6a$ persistent current, and phenocopies the *nav* mutant response to touch in wild type embryos. (A) Two electrode voltage clamp recordings from oocytes co-expressing $Na_V1.6a$ and $\beta 1$ in the absence or presence of Riluzole (50 μM) demonstrating selective blockade of the persistent sodium current. (B) Concentration–response relationship of Riluzole effect on persistent and transient sodium currents. Values represent the average ± SEM ($n = 10$). Riluzole (10 μM) mimics the *nav* behavioral response to touch (C), and the abbreviated pattern of touch-evoked synaptic drive to *nav* axial skeletal muscle in wild-type embryos (48 hpf) (D).

RBs in mutants may be sufficient to activate the M cell and the fast escape contraction but not other reticulospinal interneurons that may normally drive the swim circuit. However, prolonged suprathreshold current injection was unable to initiate a train of action potentials in wild-type RBs consistent with the possibility that tactile stimuli elicit only a transient response in RBs. Indeed, RBs responded to the onset of mechanosensory stimulation with a single action potential and offset of the stimulus with a single action potential in wild-type zebrafish embryos (unpublished results). Since intracellular injection of

current can elicit spiking in mutant RBs as in wild-type RBs, it seems unlikely that the loss of $Na_V1.6a$ unduly affects the responsiveness of mechanosensory neurons to tactile stimuli. This suggests that defects in signaling downstream of the sensory neurons account for the lack of swimming following tactile stimulation in mutants. Furthermore, the fact that exogenous NMDA elicits fictive swimming in both wild-type and *nav* mutants suggests that the swim circuit was intact in mutants but was inadequately activated. Thus, $Na_V1.6a$ might be required in neurons postsynaptic to the mechanosensory neurons and upstream of the swim circuit that normally provides excitatory drive to the swim circuit. The additional fact that the duration and intraburst frequency of the bouts of fictive swimming initiated by NMDA were lower in mutants compared with wild type suggested that $Na_V1.6a$ was also required by the swim circuit for normal swimming.

Persistant sodium currents are required in some neurons to generate bursts of action potentials and have been implicated in locomotion by mammals (Zhong et al., 2007; Tazerart et al., 2007, 2008). Zebrafish $Na_V1.6a$ exhibits persistent current that can be selectively eliminated with the drug Riluzole much like mammalian $Na_V1.6$ (Urbani and Belluzzi, 2000). Interestingly, acute application of Riluzole to wild-type embryos mimicked the aberrant touch-evoked behavior and synaptic drive to skeletal muscle observed in *nav* mutants. These pharmacological results along with the apparent requirement of $Na_V1.6a$ in interneurons upstream of the swim pattern generator are consistent with a requirement of a $Na_V1.6a$ persistent current in these upstream neurons. However, the hypothesis that $Na_V1.6a$ persistent current is required by interneurons that normally activate the swim pattern generator awaits a more complete analysis of the membrane properties of these interneurons in wild-type and mutant embryos.

We thank the members of the Kuwada and Hume labs for discussions of the experiments described in this manuscript. We also thank Dr. Lori L. Isom (University of Michigan) for providing wild-type scn8aa.

REFERENCES

Baier H. 2000. Zebrafish on the move: Towards a behavior-genetic analysis of vertebrate vision. Curr Opin Neurobiol 10:451–455.

Beattie CE, Hatta K, Halpern ME, Liu H, Eisen JS, Kimmel CB. 1997. Temporal separation in the specification of primary and secondary motoneurons in zebrafish. Dev Biol 187:171–182.

Buss RR, Drapeau P. 2000. Physiological properties of zebrafish embryonic red and white muscle fibers during early development. J Neurophysiology 84:1545–1557.

Buss RR, Drapeau P. 2001. Synaptic drive to motoneurons during fictive swimming in the developing zebrafish. J Neurophysiol 86:197–210.

Buss RR, Drapeau P. 2002. Activation of embryonic red and white muscle fibers during fictive swimming in the developing zebrafish. J Neurophysiol 87:1244–1251.

Chandrasekhar A, Shcauerte HE, Haffter P, Kuwada JY. 1999. The zebrafish detour gene is essential for cranial but not spinal motor neuron induction. Development 126:2727–2737.

Chen YH, Huang FL, Cheng YC, Wu CJ, Yang CN, Tsay HJ. 2008. Knockdown of zebrafish Nav1.6 sodium channel impairs embryonic locomotor activities. J Biomed Sci 15:69–78.

Chopra SS, Watanabe H, Zhong TP, Roden DM. 2007. Molecular cloning and analysis of zebrafish voltage-gated sodium channel beta subunit genes: Implications for the evolution of electrical signaling in vertebrates. BMC Evol Biol 7:113.

Clarke JD, Hayes BP, Hunt SP, Roberts A. 1984. Sensory physiology, anatomy and immunohistochemistry of Rohon-Beard neurones in embryos of *Xenopus laevis*. J Physiol 348:511–525.

Crill WE. 1996. Persistent sodium current in mammalian central neurons. Ann Rev Physiol 58:349–362.

Cui WW, Low SE, Hirata H, Saint-Amant L, Geisler R, Hume RI, Kuwada JY. 2005. The zebrafish shocked gene encodes a glycine transporter and is essential for the function of early neural circuits in the CNS. J Neurosci 25:6610–6620.

Cui WW, Saint-Amant L, Kuwada JY. 2004. Shocked gene is required for the function of a premotor network in the zebrafish CNS. J Neurophysiol 92:2898–2908.

Downes GB, Granato M. 2006. Supraspinal input is dispensable to generate glycine-mediated locomotive behaviors in the zebrafish embryo. J Neurobiol 66:437–451.

Drapeau P, Ali DW, Buss RR, Saint-Amant L. 1999. In vivo recording from identifiable neurons of the locomotor network in the developing zebrafish. J Neurosci Methods 88:1–13.

Eaton RC, DiDomenico R, Nissanov J. 1988. Flexible body dynamics of the goldfish C-start: Implications for reticulospinal command mechanisms. J Neurosci 8:2758–2768.

Eaton RC, Farley RD. 1975. Mauthner neuron field potential in newly hatched larvae of the zebra fish. J Neurophysiol 38:502–512.

Fashena D, Westerfield M. 1999. Secondary motoneuron axons localize DM-GRASP on their fasciculated segments. J Comp Neurol 406:415–424.

Fein AJ, Meadows LS, Chen C, Slat EA, Isom LL. 2007. Cloning and expression of a zebrafish SCN1B ortholog and identification of a species-specific splice variant. BMC Genomics 8:226.

Gahtan E, Sankrithi N, Campos JB, O'Malley DM. 2002. Evidence for a widespread brain stem escape network in larval zebrafish. J Neurophysiol 87:608–614.

Granato M, van Eeden FJM, Schach U, Trowe T, Brand M, Furutani-Seiki M, Haffter P, Hammerschmidt M, Heisenberg C-P, Jiang Y-J, Kane DA, Kelsh RN, Mullins MC, Odenthal J, Nüsslein-Volhard C. 1996. Genes controlling and mediating locomotion behavior of the zebrafish embryo and larva. Development 123:399–413.

Haffter P, Nusslein-Volhard C. 1996. Large scale genetics in a small vertebrate, the zebrafish. Int J Dev Biol 40: 221–227.

Hirata H, Saint-Amant L, Downes GB, Cui WW, Zhou W, Granato M, Kuwada JY. 2005. Zebrafish bandoneon mutants display behavioral defects due to a mutation in the glycine receptor beta-subunit. Proc Natl Acad Sci USA 102:8345–8350.

Hirata H, Saint-Amant L, Waterbury J, Cui W, Zhou W, Li Q, Goldman D, et al. 2004. *Accordion*, a zebrafish behavioral mutant, has a muscle relaxation defect due to a mutation in the ATPase Ca2+ pump SERCA1. Development 131:5457–5468.

Hirata H, Watanabe T, Hatakeyama J, Sprague SM, Saint-Amant L, Nagashima A, Cui WW, et al. 2007. Zebrafish relatively relaxed mutants have a ryanodine receptor defect, show slow swimming and provide a model of multi-minicore disease. Development 134:2771–2781.

Hukriede NA, Joly L, Tsang M, Miles J, Tellis P, Epstein JA, Barbazuk WB, et al. 1999. Radiation hybrid mapping of the zebrafish genome. Proc Natl Acad Sci USA 96:9745–9750.

Isom LL, Scheuer T, Brownstein AB, Ragsdale DS, Murphy BJ, Catterall WA. 1995. Functional co-expression of the beta 1 and type IIA alpha subunits of sodium channels in a mammalian cell line. J Biol Chem 270:3306–3312.

Jontes JD, Buchanan J, Smith SJ. 2000. Growth cone and dendrite dynamics in zebrafish embryos: Early events in synaptogenesis imaged in vivo. Nature Neurosci 3:231–237.

Kanki JP, Chang S, Kuwada JY. 1994. The molecular cloning and characterization of potential chick DM-GRASP homologs in zebrafish and mouse. J Neurobiol 25:831–845.

Kimmel CB, Ballard WW, Kimmel SR, Ullmann B, Schilling TF. 1995. Stages of embryonic development of the zebrafish. Dev Dyn 203:253–310.

Korn H, Faber DS. 2005. The Mauthner cell half a century later: A neurobiological model for decision-making? Neuron 47:13–28.

Lefebvre JL, Ono F, Puglielli C, Seidner G, Franzini-Armstrong C, Brehm P, Granato M. 2004. Increased neuromuscular activity causes axonal defects and muscular degeneration. Development 131:2605–2618.

Li Q, Shirabe K, Kuwada JY. 2004. Chemokine signaling regulates sensory cell migration in zebrafish. Dev Biol 269:123–136.

McDearmid JR, Liao M, Drapeau P. 2006. Glycine receptors regulate interneuron differentiation during spinal network development. Proc Natl Acad Sci USA 103:9679–9684.

Meisler MH, Kearney JA, Sprunger LK, MacDonald BT, Buchner DA, Escayg A. 2002. Mutations of voltage-gated sodium channels in movement disorders and epilepsy. Novartis Foundation Symp 241:72–81; discussion82–76:226–232.

Metcalfe WK, Myers PZ, Trevarrow B, Bass MB, Kimmel CB. 1990. Primary neurons that express the L2/HNK-1 carbohydrate during early development in the zebrafish. Development 110:491–504.

Nissanov J, Eaton RC, DiDomenico R. 1990. The motor output of the Mauthner cell, a reticulospinal command neuron. Brain Res 517:88–98.

Novak AE, Jost MC, Lu Y, Taylor AD, Zakon HH, Ribera AB. 2006a. Gene duplications and evolution of vertebrate voltage-gated sodium channels. J Mol Evol 63:208–221.

Novak AE, Taylor AD, Pineda RH, Lasda EL, Wright MARibera AB. 2006b. Embryonic and larval expression of zebrafish voltage-gated sodium channel alpha-subunit genes. Dev Dyn 235:1962–1973.

Ono F, Mandel G, Brehm P. 2004. Acetylcholine receptors direct rapsyn clusters to the neuromuscular synapse in zebrafish. J Neurosci 24:5475–5481.

Ono F, Shcherbatko A, Higashijima S, Mandel G, Brehm P. 2002. The Zebrafish motility mutant twitch once reveals new roles for rapsyn in synaptic function. J Neurosci 22: 6491–6498.

Pineda RH, Heiser RA, Ribera AB. 2005. Developmental, molecular, and genetic dissection of INa in vivo in embryonic zebrafish sensory neurons. J Neurophysiol 93: 3582–3593.

Pineda RH, Svoboda KR, Wright MA, Taylor AD, Novak AE, Gamse JT, Eisen JS, et al. 2006. Knockdown of Nav1.6a Na+ channels affects zebrafish motoneuron development. Development 133:3827–3836.

Postlethwait JH, Johnson SL, Midson CN, Talbot WS, Gates M, Ballinger EW, Africa D, et al. 1994. A genetic linkage map for the zebrafish. Science 264: 699–703.

Raman IM, Sprunger LK, Meisler MH, Bean BP. 1997. Altered subthreshold sodium currents and disrupted firing patterns in Purkinje neurons of Scn8a mutant mice. Neuron 19:881–891.

Ribera AB, Nusslein-Volhard C. 1998. Zebrafish touch-insensitive mutants reveal an essential role for the developmental regulation of sodium current. J Neurosci 18:9181–9191.

Saint-Amant L, Drapeau P. 1998. Time course of the development of motor behaviors in the zebrafish embryo. J Neurobiol 37:622–632.

Tazerart S, Viemari JC, Darbon P, Vinay L, Brocard F. 2007. Contribution of persistent sodium current to locomotor pattern generation in neonatal rats. J Neurophysiol 98:613–628.

Tazerart S, Vinay L, Brocard F. 2008. The persistent sodium current generates pacemaker activities in the central pattern generator for locomotion and regulates the locomotor rhythm. J Neurosci 28:8577–8589.

Trevarrow B, Marks DL, Kimmel CB. 1990. Organization of hindbrain segments in the zebrafish embryo. Neuron 4:669–679.

Tsai CW, Tseng JJ, Lin SC, Chang CY, Wu JL, Horng JF, Tsay HJ. 2001. Primary structure and developmental expression of zebrafish sodium channel Na(v)1.6 during neurogenesis. DNA Cell Biol 20:249–255.

Urbani A, Belluzzi O. 2000. Riluzole inhibits the persistent sodium current in mammalian CNS neurons. Eur J Neurosci 12:3567–3574.

Zhong G, Masino MA, Harris-Warrick RM. 2007. Persistent sodium currents participate in fictive locomotion generation in neonatal mouse spinal cord. J Neurosci 27:4507–4518.

Zhou W, Saint-Amant L, Hirata H, Cui WW, Sprague SM, Kuwada JY. 2006. Non-sense mutations in the dihydropyridine receptor beta1 gene. CACNB1, paralyze zebrafish relaxed mutants. Cell Calcium 39:227–236.

Zottoli SJ. 1977. Correlation of the startle reflex and Mauthner cell auditory responses in unrestrained goldfish. J Exp Biol 66:243–254.

Zottoli SJ, Faber DS. 1979. Properties and distribution of anterior VIIIth nerve excitatory inputs to the goldfish Mauthner cell. Brain Res 174:319–323.